# Pulsed Power for Lunar Applications

Ian R. McNab, *Life Fellow, IEEE*, and Kristin R. Enzenauer

***Abstract*— Under the Artemis program, National Aeronautics and Space Administration (NASA) plans to establish and develop a permanently manned settlement on the Moon over the next decade. Electrical power is a vital resource for a sustainable lunar base, and photovoltaic arrays plus a small (10 kW) fission power plant will be used for the base power generation. The preferred location for the base is at the south pole of the Moon near a crater that offers access to sunlight for solar power, line-of-sight communications to Earth, and low temperature permanently shadowed regions (PSRs) that contain lunar ice and other resources for self-sustainment. The PSR regions are below the critical operating temperature of modern "high" temperature superconductors (HTSs) and we, therefore, suggest that an HTS superconducting magnetic energy storage (SMES) system could provide MJ, MW pulsed power to support the Artemis habitat. Lunar pulsed power requirements could include directed energy systems, high power radars, and electromagnetic (EM) launch systems for lunar detection and defense against meteorites, as well as lunar surveying and global positioning system (GPS), and lunar manufacturing. An SMES system has moderate energy storage density but high-power density, fast discharge times, and high efficiency. It is inherently long-lasting, ideally suited to the low PSR temperatures, and uses environmentally acceptable materials.**

***Index Terms*— Lunar, power, superconducting, superconducting magnetic energy storage (SMES).**

## I. INTRODUCTION

THIS year marks 50 years since astronauts last set foot on the Moon with the Apollo program. National Aeronautics and Space Administration (NASA) intends to reset this timeline by landing astronauts on the lunar surface in 2025 under the Artemis program [1]. The goals of the Artemis program are to land the first woman and first person of color on the Moon, to establish a permanent lunar settlement known as the Artemis base camp, and to demonstrate the technological capability required for future space exploration including a Mars landing [2]. The four astronauts selected for the first lunar orbital flight have already been announced.

To help meet these objectives, NASA will establish a permanently orbiting space station known as the Gateway (Fig. 1) in a near-rectilinear halo orbit around the Moon and Lagrange point 2 (L2) that will serve as a staging point for human and robotic lunar mission. Lunar resources and supplies will be transported to and from the Gateway to the Artemis Base Camp to maintain the lunar base, facilitate exploration, and eventually support a mission to Mars.

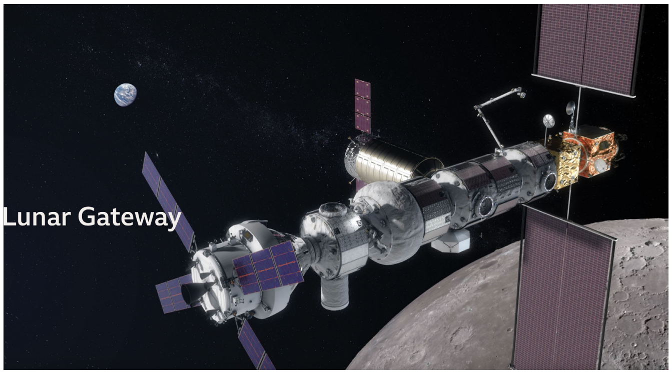

Fig. 1. Gateway space station [1].

NASA's plan is to generate baseload electrical power for the Artemis base camp with advanced solar panels and a small, lightweight fission power system [1]. In addition to lunar base load power, there is also a potential need for short-term, pulsed power for various applications such as pulsed high-power radars, directed energy systems, and electromagnetic (EM) launch systems for the detection and defense against meteorite threats, as well as lunar surveying and global positioning system (GPS), and lunar manufacturing. For example, a previous study evaluated a lunar EM mass accelerator (LEMMA) as an alternative to chemical rockets to enable the transportation of materials from the Artemis base camp to the Gateway [3], [4], while a lunar-based defense against Earth threats from asteroids or comets has been suggested [5].

This study has evaluated the use of a superconducting magnetic energy storage (SMES) system based on modern high temperature superconductors (HTSs) made from doped copper oxide perovskite materials to supplement the baseload power with MJ, MW pulsed power. SMES provides a quick response to a high energy demand with an energy transfer efficiency up to 95%. A SMES stores energy in the magnetic field created by the current flowing through superconductors that are formed into a large solenoidal or toroidal magnet. After the superconducting coil has been energized from a direct current (dc) source, it stores the energy permanently without losses until the coil is commanded to discharge into a load. Depending on the load requirements, the power conditioning system (PCS) can either convert the coil dc to alternating current (ac) at the required frequency or transform it into higher dc voltage or current. The power output of a SMES system can range from kW to MW with a response time of milliseconds, making it beneficial for rapid, pulsed power required by applications such as LEMMA [3], [4]. A SMES system can also help to stabilize the frequency and

---

Manuscript received 12 September 2023; revised 27 September 2023; accepted 4 October 2023. Date of publication 26 October 2023; date of current version 9 December 2024. The review of this article was arranged by Senior Editor R. P. Joshi. *(Corresponding author: Ian R. McNab.)*

The authors are with the Physics Department, Naval Postgraduate School, Monterey, CA 93943 USA (e-mail: ian.mcnab@nps.edu).

Color versions of one or more figures in this article are available at https://doi.org/10.1109/TPS.2023.3322632.

Digital Object Identifier 10.1109/TPS.2023.3322632

U.S. Government work not protected by U.S. copyright.

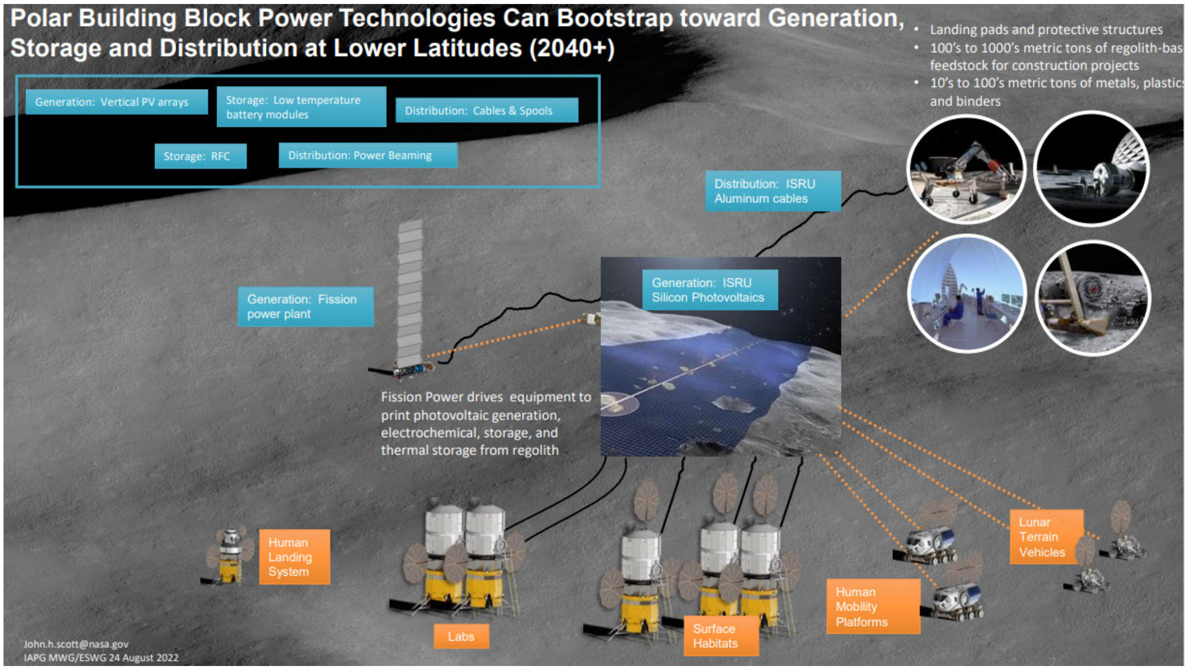

Fig. 2. Notional lunar power grid (from [8]).

voltage of the Artemis Base Camp power grid by operating as a flexible ac transmission system to inject stabilizing power pulses automatically when required [6].

For a SMES system to operate properly, the magnetic coils must be kept at a temperature below the critical temperature of the superconducting material to stay in the superconducting state. On Earth, to achieve and maintain the required low temperatures, a refrigerator must be used with an appropriate cryogen and the magnetic coil must be kept within an insulated cryostat. Low temperature superconductors (LTS) such as NbTi or $Nb_3Sn$ need to be kept at or below liquid helium liquification temperatures (<4 K) to remain superconducting but newer HTS can operate at up to liquid nitrogen temperatures (77 K). Temperatures below this exist on the Moon in permanently shadowed regions (PSRs) of lunar craters at the Moon's south pole, and elsewhere. It is, therefore, possible that an HTS SMES system can operate stably without the need for an expensive refrigeration system if it is placed within a lunar crater. NASA's Lunar Reconnaissance Orbiter has measured the coldest temperatures in the solar system inside these craters, with temperatures dropping below 40 K [7].

## II. Lunar Base Camp Power

NASA is considering potential sites for the Artemis Base Camp. Factors involved in choosing the optimum site include.

1) Access to sunlight for solar power generation.
2) Direct line-of-sight to Earth for communications.
3) Vicinity to PSRs that contain lunar ice and other volatiles.

Because the Moon's axis tilts only 1.5° relative to the ecliptic (versus 23.5° for the Earth), the poles receive sunlight all year and are also visible from the Earth. Areas near the Shackleton Crater at the South Pole are therefore currently considered the primary choice for the Artemis base camp. A base camp on a crater rim, will remain illuminated and have line-of-sight access to Earth while having PSRs with temperatures below 50 K that contain useful volatile resources, including lunar ice.

One of the first priorities for a lunar habitat is to establish a self-sufficient power grid. NASA plans to use solar cells and fission power to generate power for the grid system. Fig. 2 shows a suggested arrangement [8]. This will support the astronaut's lunar habitat with house-keeping requirements – air circulation, heating/cooling, lighting, food preparation, communications, controls, and diagnostics. It will also provide recharge capability for batteries used in vehicles, power tools, communications, etc. Superconducting power distribution cables could be used if they can be shielded and cooled.

## III. Pulsed Power

It can be expected that pulsed power will be needed on the Moon for several applications. It is too early to know with any certainty what power levels may be needed but it can be anticipated that early systems may need up to kilovolt, kA pulses of sub-seconds to seconds to support the type of applications mentioned below. As an increasing energy infrastructure becomes established on the Moon, these requirements may be expected to increase.

Possible applications could include.

1) Pulsed radars and high energy laser systems for the detection and elimination of incoming meteorites that threaten human habitats or critical equipment. There is no lunar atmosphere to help shield against small, high velocity threats. The Earth's defenses could also benefit from lunar-based radars and defense systems [5].
2) High power pulsed communications with Earth, the Gateway, and Mars missions.

3) EM launch of sub-orbital reconnaissance/survey flights to provide aerial surveys of the lunar surface to assess local conditions, including in situ resources, such as water and minerals that provide raw materials to support permanent human habitations.
4) EM launch of satellites into low lunar orbit (LLO) to provide lunar-wide telecommunications and navigation capability by a system of satellites and ground stations like those in low Earth orbit (LEO) for the Earth.
5) EM launch of ice or $LH_2$ to the Gateway to support the Mars mission [3], [4], [9].
6) EM launch of lunar materials to other cis-lunar or near-Earth habitats [10].
7) The lunar power grid may benefit from short duration high power stabilization.
8) Some mining and fabrication processes may also require intermittent high-power pulses [11], [12].

Regarding items 3–5, the lunar orbital velocity at an altitude of 200 km is 1.6 km/s and lunar escape velocity is 2.38 km/s. Both are within the capability of railguns, which alone amongst EM launch techniques are capable of high velocity launch. Given the lack of an atmosphere, and hence aerothermal heating, EM launch can be expected to be particularly appropriate for lunar operation. EM launch systems will not pollute the lunar environment with exhaust plumes of lunar regolith dust, as with chemical rockets. Because of low lunar gravity, such dust plumes are slow to dissipate and contaminate wide areas of the landscape, causing a problem for human habitats and support equipment.

Options for storing energy and delivering power pulses include capacitors, flywheels, batteries, fuel cells/fuel, and SMES. The Ragone plot is often used to compare specific energy and specific power for various technologies. Batteries and ultracapacitors are usually very good at storing energy–i.e., they have very high energy density–but usually have poor power delivery because of their inherently low voltage. Conversely, electrostatic capacitors operate at high voltage and have very high-power density ratings but a low energy density. High speed flywheels are usually intermediate: they require bearings and safety considerations, and torque management is required during discharge. SMES has moderate energy density but high-power delivery capability, as illustrated in Fig. 3 [13].

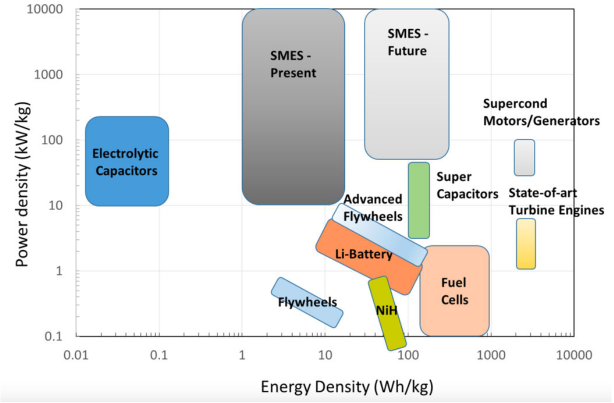

Fig. 3. Ragone plot [13].

## IV. HTS SMES

The basic feature of an SMES is that energy is stored without losses in the magnetic field associated with the current in a superconducting electrical conductor. For an inductor, the energy stored is $E = LI^2/2$, where $L$ is inductance and $I$ is current, and the energy density of the magnetic field of an air-cored inductor is

$$E_D = \frac{B^2}{2\mu_0}. \tag{1}$$

For $B = 10$ T, $E_D = 40$ MJ/m$^3$ and for $B = 20$ T, $E_D = 160$ MJ/m$^3$.

The basic components of an SMES system are shown in Fig. 4 and are as follows.

1) The superconducting coil (inductor).

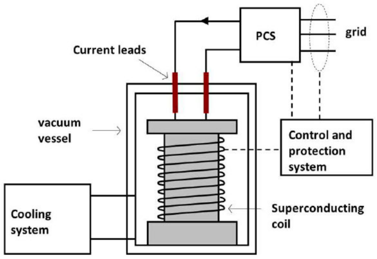

Fig. 4. SMES system components [6].

2) The cryostat and refrigeration system.
3) Low-to-high temperature current transition leads.
4) The PCS.
5) Controls and instrumentation.

For an SMES system to operate properly, the magnetic coils must be kept at very low temperatures to stay in a superconducting state: this requires a refrigerator to cool all the components within the cryostat. New HTS can operate at and even above liquid nitrogen liquification temperatures (77 K), much higher than the prior LTS that required 4 K or lower. It is possible that this cooling requirement for an HTS SMES system can be achieved without a refrigeration system if it is placed within the PSR of a lunar crater.

Several inductor variants are possible, with the simplest being a solenoid and the most complex being a toroid. The solenoid uses the least amount of expensive superconductor, but the disadvantage is that it creates a magnetic field that can propagate over a wide area, especially when operated at high magnetic field, as desired for storing high energies. This can affect nearby electrical and electronic equipment and create unwanted forces on metallic objects and structures. The toroidal geometry largely overcomes the field fringing concern, but typically requires two to three times the amount of superconductor. Some examples of coil geometries are shown in Fig. 5 [14], [15], [16]. Magnetic field fringing can be reduced progressively with a dual opposing coil geometry, and a four or six coil arrangement, as shown on the top and center rows. The toroidal geometry on the lower left is the best while the "bumpy torus" shown at the lower center approximates that behavior using multiple solenoidal coils. The dee-shaped coil

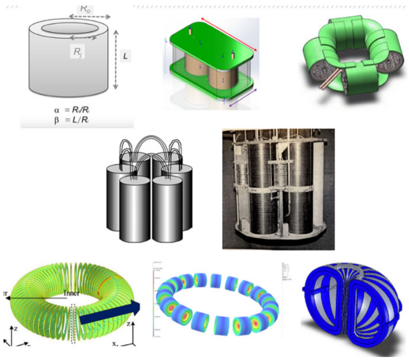

Fig. 5. Alternative inductor geometries [14], [15], [16].

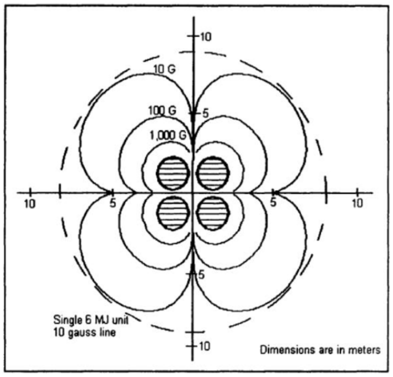

Fig. 6. Comparison of fringing fields for four solenoids versus a single solenoid [17].

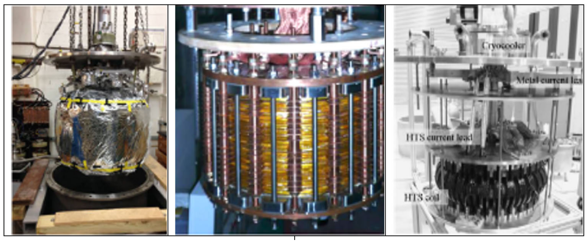

Fig. 7. Recent HTS coils [18], [19], [20].

cross section shown on the lower right is the optimum shape for a toroidal coil, as used in modern thermonuclear fusion containment magnet assemblies. The benefit of using multiple opposed coils was studied by Weinstock [17] as exemplified in Fig. 6 where the fringing fields of four 6 MJ opposed coils are compared with the 0.001 T (10 G) field line of a single 6 MJ solenoid.

Three recent HTS coils that have been fabricated and tested are shown in Fig. 7. The 25-kJ coil on the left was built by the NDI Engineering Company and tested at the University of Wisconsin [18], the center one was built by Huazhong University and used a hybrid construction with bismuth strontium calcium copper oxide (BSSCO) and yttrium barium copper (YBCO) coils [19], while the one on the right was a toroidal configuration developed in South Korea [20]. All three coils validated the design and fabrication processes at some level. Testing showed that careful consideration of electrical, mechanical, and thermal design features are all necessary to ensure success. Depending on the location of a SMES system on the Moon, the need for minimizing the fringing magnetic field will have to be assessed. The toroidal design is likely to be more expensive and use more superconductor for a given energy storage than a solenoidal coil.

In addition to the inductor, important SMES system components include the cryogenic-to-ambient temperature transition leads. For terrestrial use, these can be permanently connected or disconnectable to reduce thermal losses. In a PSR lunar crater, the permanently connectable option is likely to be preferred since it eliminates any unreliability caused by repeated connecting and disconnecting the conducting joint. In terrestrial applications, the PCS is usually operated at ambient temperature although some organizations have advocated locating the electronics in the cryostat to take advantage of reduced Ohmic losses [21]. In a lunar PSR location, operation at cryogenic temperatures is preferred to minimize losses; suitable electronic components will need to be chosen for this operating regime since not all materials benefit from low temperature operation.

In many cases, the load current is usually the same as the coil current, but inverters go from dc/ac for utility grid applications. If high currents are needed for some applications, such as EM launch, a dc/dc transformer may be needed. Taking advantage of the PSR temperatures, it would be also appropriate for this to also use HTS material.

## V. SUPERCONDUCTING OPTIONS

The strange phenomenon of superconductivity was discovered unexpectedly by Kamerlingh-Onnes in 1911 when he cooled a sample of mercury wire to 4 K using liquid helium that he had recently learned to liquify [22]. A handful of other materials were discovered in subsequent decades, but the phenomenon remained largely a laboratory curiosity until the 1960's when niobium alloys were discovered and, over the next decade or two, developed into engineering materials that could be produced reliably and in large quantities. Today, the global superconductivity business is about $7 B/year, with almost all of that being based on LTS NbTi alloy wire [23]. About 80% (approximately $5 B) of the market is dominated by medical applications using nuclear magnetic resonance imaging (MRI) equipment. About 36 000 machines of this type are in operation globally, mostly in the USA, Japan, and Europe, and a further 3000 are manufactured each year. These machines have sophisticated designs featuring increasingly higher operating fields – from 1.5 to 3 to 7 T and now 11.2 T [24] – sophisticated gradient techniques, and, recently, greatly reduced LHe content in sealed systems [25]. Additional users of LTS materials include national and international high energy particle physics accelerator research programs, such as European Organization for Nuclear Research (CERN) which has over 1500 superconducting magnets, and thermonuclear fusion research experiments, such as International Thermonuclear Experimental Reactor (ITER), for which the 18-magnet toroidal plasma confinement magnets will store 44 GJ. Japanese and Chinese Maglev high speed trains also use LTS propulsion, levitation, and guidance systems.

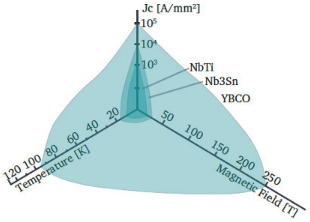

Fig. 8. Comparison of YBCO and titanium alloy superconductors [27].

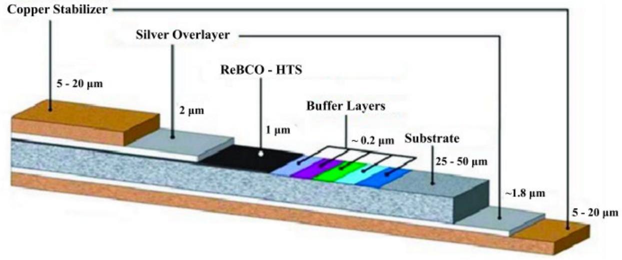

Fig. 9. Structure of a typical HTS ReBCO tape [27].

A new class of superconductors was discovered by Bednorz and Muller [26]. These were based on doped perovskite copper oxide crystals and operated at much higher operating critical temperatures ($T_c$), current densities ($J_c$), and magnetic field strengths ($H_c$) than Nb alloys (Fig. 8).

This discovery energized the field of superconductivity and reawakened hopes of finding room temperature superconductors, which would revolutionize the world economy. Since then, many more HTS materials have been discovered and operating temperatures above liquid nitrogen temperatures have been established and hints of room temperature operation have even been claimed, albeit at extraordinarily high pressures. Most focus now is on second-generation materials based on rare earth doped barium copper oxide (ReBCO). The crystalline structure of ReBCO is more difficult to fabricate than NbTi, requiring substrates and special techniques but lengths up to 1 km are now available. The HTS field is vigorous, and discoveries continue at a rapid pace.

Emerging areas that can benefit from these materials include all-electric and hybrid aircraft as well as utility power generation, wind power generators, motors, and distribution, and commercial thermonuclear fusion ventures. These, plus the medical imaging community, can provide high investments that are likely to drive HTS progress. The Advanced Research Projects Agency-Energy (ARPA-E) has recently announced a program to reduce the cost of US-manufactured HTS tape by a factor of ten, which is expected to further encourage users.

For this study, we have assumed that existing ReBCO materials could be used for a lunar SMES system. Such materials are made in the form of micrometer-thick layers deposited on a specially textured 4- or 12-mm wide Hastalloy base, surrounded by silver and a copper stabilizer layer (Fig. 9) [27]. The HTS tape is anisotropic and more difficult to wind than NbTi wire. Cabling multiple tapes together with little or no insulation reduces anisotropy, increases current ($I$) and minimizes the number of turns ($N$) for a given magnet $NI$. It also minimizes or potentially eliminates quench sensitivity (Fig. 10).

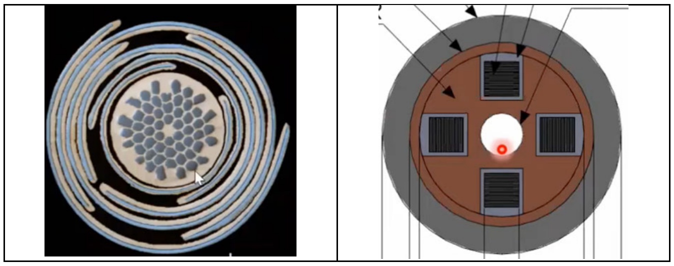

Fig. 10. HTS cable concepts [28], [29].

## VI. HTS SMES LOCATION

To be of value, the SMES system should be placed relatively close to the Artemis Base Camp and the cryostat should be buried in a PSR to leverage the cold ambient temperature and minimize the cooling requirements. Fig. 11 shows average temperatures near the lunar south pole [30]. Maximum temperatures are about 20 K higher but still within the operating range of ReBCO materials.

Embedding the SMES system in the regolith will significantly reduce the cooling requirement and offer protection against micrometeorite impact and cosmic and solar radiation [31]. If a site in the very large and deep Shackleton Crater (Fig. 12) is chosen [32], careful consideration will need to be given to safety aspects if NASA's lunar terrain vehicles (LTVs) are operated on the steep crater slope. Solar power located on the crater rim could charge the SMES via a zero-loss HTS superconducting cable, as suggested by Evans and Ignatiev (Fig. 13) [33].

## VII. SMES HEAT DISSIPATION

The advantage of embedding the HTS SMES in the low temperature lunar regolith can be estimated from a simple calculation of the dissipation of generated heat into the regolith.

A variety of estimates for the thermal properties of the lunar regolith are available, based on a limited amount of experimental data obtained with lunar landers after fitting with various models. Less is available for the low temperature PSR areas, but estimates are available and have been used here.

One way to assess the advantages of burying the cryostat within a lunar crater is to assess how the temperature of the regolith changes after the SMES system releases heat during a high energy pulse. This can be calculated using the following equation:

$$Q = mC\Delta T \tag{2}$$

where $Q$ = heat transferred ($W$), $m$ = mass (kg), $C$ = specific heat capacity (J/kg.K), and $\Delta T$ = temperature change ($K$).

Assuming arbitrarily for this estimate that the cryostat is a cylinder 2 m in diameter and 2 m tall and that the heat generated during a SMES pulse is 300 W that is uniformly dissipated into a volume of regolith that is 1 m larger in diameter than the cryostat, the total volume of regolith in which heat will be dissipated is 18.85 $m^3$. Multiplying the

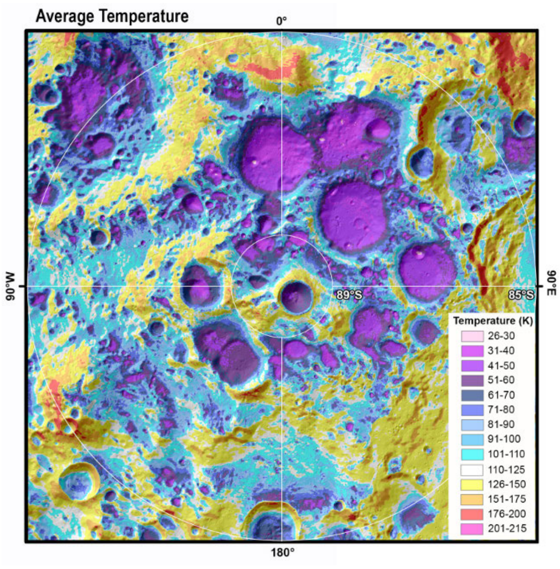

Fig. 11. Average temperatures near the lunar south pole [30].

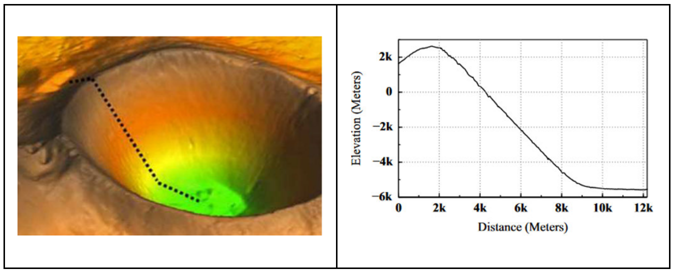

Fig. 12. Shackleton crater [31].

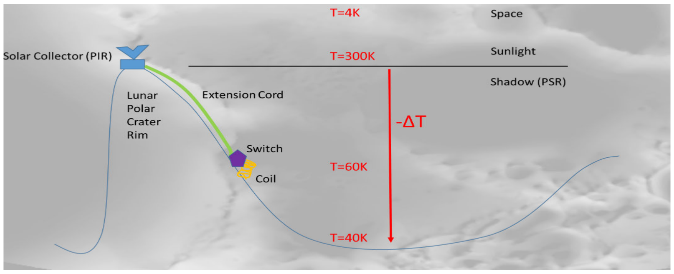

Fig. 13. Possible SMES location [33].

volume by the density of the regolith, 1500 kg/m$^3$, gives the total mass of the regolith to be approximately 28 275 kg. The specific heat of the regolith at 40 K is 86 J/kg.K using the equations derived by [34]. Substituting these values into (2), gives the total temperature rise of the regolith to be 0.0001 K. This very low temperature rise demonstrates that any heat generated during the SMES operation should be easily absorbed into the regolith, even if our assumptions are uncertain.

In (2), we assumed that the heat generated by the SMES energy pulsed was dissipated into the region around the cryostat. To do this it is necessary to conduct the heat into the regolith. The conduction of heat is determined by the following equation:

$$Q = kA\left(\frac{\Delta T}{L}\right)t \tag{3}$$

where $Q$ = heat transferred $(W)$, $k$ = thermal conductivity (W/mK), $L$ = thickness $(m)$, $A$ = area (m$^2$), $\Delta T$ = hot–cold temperature differential $(K)$, and $t$= time $(s)$.

With the assumed cryostat outer dimensions, the surface area is 18.85 m$^2$. The temperature gradient between the wall of the cylinder and the lunar regolith is assumed to be 37 K (77 K at cylinder wall, and 40 K in lunar regolith). Substituting these values, along with a value of thermal conductivity at one meter depth of 0.00884 W/m.K [35] into (3), shows that it will take about 48 s for 300 W of heat to be dissipated into a 1 m thickness of the lunar regolith surrounding the cryostat. If this is not adequate to support pulsed operation, the time can be decreased by increasing its surface area of the cylinder by adding fins or using heat pipes to transfer the heat into a larger regolith volume.

It is too early to perform more detailed calculations at present, but these estimates validate the concept of embedding the cryogenic system within the lunar regolith in a crater PSR. Placing the SMES system on the lunar surface would eliminate this benefit and significantly reduce the cooling capability. More detailed calculations using more accurate regolith data, when it becomes available, can be used to validate these results.

## VIII. ELECTROMAGNETIC LAUNCH

Operating an EM launcher on the Moon has two important advantages compared with the Earth. First, there is no significant atmosphere, so drag and aerothermal heating of the launched projectile are not issues that need to be considered. A consequence of this is that simple calculations can be used to estimate flight trajectories. Second, the lunar gravity is much lower than Earth's–about 1.62 m$^2$/s compared with 9.81 m$^2$/s, so it is much easier to achieve higher velocities with a given force–or a given velocity with lower force.

As an example, we can estimate what might be required to achieve orbital velocity at an altitude of 200 km, where the orbital velocity is about 1.6 km/s.

For a projectile launched with an initial velocity $V_0$ and an angle $\propto$ to the horizontal, the horizontal component of velocity is

$$V_x = V_0 \cos \propto \tag{4}$$

and the vertical component is

$$V_y = V_0 \sin \propto . \tag{5}$$

The maximum height of the parabolic trajectory is

$$h_{\max} = \frac{V_y^2}{2g}. \tag{6}$$

We require $h_{\max}$ to be 200 km so inserting $g = 1.62$ m/s$^2$ yields $V_y = 805$ m/s. At this altitude, we require the projectile to have the orbital velocity, $V_x$, of 1600 m/s. Putting this value in (4) we can then solve with (5) to find the required launch angle of 26.8°. The resulting required launch velocity is 1664 m/s. Under these conditions, the launched mass will reach the required altitude with the required orbital velocity. At that point, a small thruster rocket will circularize the orbit and to prevent the payload from falling back to the lunar surface.

For a simple constant force railgun with an efficiency of 50%, an estimate of the driving current required in the railgun can be obtained from

$$I = V_0\sqrt{\frac{m}{sL'}} \tag{7}$$

where $m$ is the mass launched, $s$ is the launcher length, and $L$' is the launcher inductance gradient. Assuming a total launch mass of 4 kg (1.5 kg for a CubeSat, 1.5 kg for an orbit circularization rocket, and 1 kg for armature and support), a launcher length of 10 m, and an inductance gradient of $10^{-6}$ H, as appropriate for a singly augmented launcher, yields a launch current of 1.05 MA, and a back EMF of 1.75 kV, both of which are well within the capability of existing small railgun launchers. More detailed estimates remain to be done but it seems feasible that a CubeSat microsatellite with, for example, remote imaging survey capability could fit within a mass budget not dissimilar to this. The average launch acceleration would be $1.38 \times 10^5$ m/s$^2$ (14.1 kilogees), which is much larger than experienced by CubeSats launched by rockets but lower than other electronic components that have been launched successfully. Hardening the CubeSat electronics for launch would be required only for the launch duration of about 12 ms.

Although the required railgun voltage level is within values that have been demonstrated in SMES systems, the current required for the simple railgun launcher evaluated above is well above values that have been delivered by SMES systems yet built. Combining the SMES with a current multiplication concept such as the Meatgrinder using a superconducting transformer may enable this to be achieved. Several developments of such transformer systems have been reported [36], [37] and similar concepts using a superconducting transformer driven by pulsed magnetohydrodynamics (MHD) generators have also been discussed [38].

## IX. CONCLUSION

A moderate number of LTS and HTS SMES systems have been successfully designed, built, and tested during the last 40 years. The main focus has been to stabilize utility power grids against surges and interruptions by injecting rapid (milliseconds to <1 s) power pulses, but MJ, MW pulsed power applications are feasible. Unlike flywheels, SMES systems are passive, inherently reliable, and do not involve noxious chemicals or disposal/contamination issues like batteries, which would also require heaters for lunar operation.

HTS material has much better performance than LTS wire and can operate up to at least LN$_2$ temperatures. It is becoming more widely available and, although presently more expensive than LTS wire, focused efforts are now being devoted to substantial cost reductions [39].

The PSR of a lunar crater seems to be an ideal location for an SMES system and should significantly reduce refrigeration loads. A remotely sited SMES, coupled to the lunar habitat by an HTS cable, will not need to minimize fringing magnetic fields, so that simple low-cost solenoids could be used.

For the next step, more detailed design studies should be undertaken in conjunction with NASA planning studies to define the characteristics of an SMES pulsed power design. Given the present very high cost of placing material on the Moon, the design will probably need to be optimized for minimum mass.

## REFERENCES

[1] *Artemis Plan: NASA's Lunar Exploration Program Overview*. Accessed: Jul. 17, 2022. [Online]. Available: https://www.nasa.gov/sites/default/files/atoms/files/artemis_plan-20200921.pdf

[2] B. Dunbar, "What is Artemis?" NASA, Tech. Rep., Jul. 2019. [Online]. Available: [Online]. Available: http://www.nasa.gov/what-is-artemis

[3] I. R. McNab and B. T. McGlasson, "Lunar electromagnetic mass accelerator (LEMMA): An initial concept assessment," *IEEE Trans. Plasma Sci.*, vol. 50, no. 10, pp. 3326–3333, Oct. 2022.

[4] H. D. Beemer and I. R. McNab, "Launch parameters of a lunar ice payload traveling via electromagnetic mass accelerator," *Acta Astronautica*, vol. 207, pp. 24–32, Jun. 2023.

[5] P. J. Turchi, "Going to the Moon to protect Earth," Letter to the Editor, Aerosp. America, Aerosp. Amer., Reston, VA, USA, Tech. Rep., p. 3, Jun. 2021.

[6] P. Tixador, "Superconducting magnetic energy storage: Status and perspective," in *Proc. IEEE/CSC ESAS Eur. Supercond. News Forum*, no. 3, 2008, p. 14.

[7] S. Shekhtman, "In dark, polar Moon craters, water not invincible, scientists argue," NASA, NASA Goddard Space Flight Center, Greenbelt, MD, USA, Tech. Rep., Jul. 2019. [Online]. Available: http://www.nasa.gov/feature/goddard/2019/inside-dark-polar-moon-craters-water-not-as-invincible-as-expected-scientists-argue

[8] J. H. Scott, "NASA's technology priorities for lunar surface power," presented at the Interagency Advanced Power Working Group, Aug. 2022.

[9] S. K. Borowski, D. R. McCurdy, and T. W. Packard, "Nuclear thermal propulsion (NTP): A proven growth technology for human NEO/Mars exploration missions," in *Proc. IEEE Aerosp. Conf.*, Mar. 2012, pp. 1–20, doi: 10.1109/AERO.2012.6187301.

[10] M. Ehresmann, R. A. Gabrielli, G. Herdrich, and R. Laufer, "Lunar based massdriver applications," *Acta Astronautica*, vol. 134, pp. 189–196, May 2017, doi: 10.1016/j.actaastro.2017.02.007.

[11] A. Ellery, "Leveraging in situ resources for lunar base construction," *Can. J. Civil Eng.*, vol. 49, no. 5, pp. 657–674, May 2022, doi: 10.1139/cjce-2021-0098.

[12] A. Ellery, "Generating and storing power on the moon using in situ resources," *Proc. Inst. Mech. Eng., G, J. Aerosp. Eng.*, vol. 236, no. 6, pp. 1045–1063, May 2022.

[13] T. J. Haugan, "Development of superconducting-magnetic energy-storage (SMES) for aerospace applications," presented at the Int. Magnet Technol. Conf. (MT), Vancouver, BC, Canada, Sep. 2019.

[14] W. Weck, P. Ehrhart, A. Müller, and G. Reiner, "Superconducting inductive pulsed power supply for electromagnetic launchers: Design aspects and experimental investigation of laboratory set-up," *IEEE Trans. Magn.*, vol. 33, no. 1, pp. 524–527, Jan. 1997.

[15] W. Weck, P. Ehrhart, A. Müller, H. Scholderle, and E. Sturm, "Demonstration of a superconducting inductive pulsed power supply at simulated load conditions," *IEEE Trans. Magn.*, vol. 35, no. 1, pp. 383–387, Jan. 1999.

[16] R. Gupta et al., "Design, construction and testing of a large aperture high field HTS SMES coil," *Trans. Appl. Supercond.*, vol. 26, no. 4, Jun. 2016.

[17] H. Weinstock, Ed., *Applications of Superconductivity*. Loen, Norway: NATO Advanced Study Institute on Applications of Superconductivity, Kluwer Academic Publishers, Jun. 1997, p. 438.

[18] O. Christianson et al., "Pulsed HTS coil performance," *IEEE Trans. Appl. Supercond.*, vol. 27, no. 4, pp. 1–4, Jun. 2017.

[19] S. Guo et al., "Study on energy storage magnet state assessment method considering temperature rise," *IEEE Trans. Appl. Supercond.*, vol. 31, no. 2, pp. 1–11, Mar. 2021.

[20] K. Kim et al., "Analysis of operational loss characteristics of 10 kJ class toroid-type SMES," *IEEE Trans. Appl. Supercond.*, vol. 21, no. 3, pp. 1340–1343, Jun. 2011.

[21] A. Elwakeel, N. McNeill, R. Pena-Alzola, M. Zhang, and W. Yuan, "Cryogenic DC/DC converter for superconducting magnet application," *IEEE Trans. Appl. Supercond.*, vol. 32, no. 6, pp. 1–5, Sep. 2022.

[22] D. van Delk and P. Kes, "The discovery of superconductivity," *Phys. Today*, vol. 63, no. 9,p. 38, Sep. 2010.

[23] M. N. Wilson, "A century of superconducting technology," *AIP Conf.*, vol. 1435, pp. 11–35, Jun. 2012.

[24] *ISEULT Project—11.7 Teslas: The World Record Magnetic Field Generated by a Human MRI Magnet*, CEA Press Release, At. Energy Commission (CEA), Paris-Saclay, 18, Jul. 2019.

[25] *For a Description of the BlueSeal Technology*. Accessed: 2023. [Online]. Available: https://www.usa.philips.com

[26] J. G. Bednorz and K. A. Mueller, "ChemInform abstract: Perovskite-type oxides—The new approach to high-tc superconductivity," *ChemInform*, vol. 19, no. 30, pp. 424–457, Jul. 1988.

[27] T. Mulder, "Advancing REBCO-CORC wire and cable-in-conduit conductor technology for superconducting magnets," Ph.D. dissertation, Faculty Sci. Technol., Univ. Twente, The Netherlands, Sep. 2018.

[28] E. Galstyan, et. al. "High critical current STAR wires with REBCO tapes by advanced MOCVD," *Supercond. Sci. Technol.*, vol. 36, 2023, Art. no. O55007.

[29] E. E. Salazar, "Quench dynamics testing and 3D modeling of VIPER HTS cable," Presented at the 27th Int. Conf. Magnet Technol., Fukuoka, Japan. Cambridge, MA, USA: MassachuseNs Institute of Technology Nov. 2021.

[30] J. Stopar, "Near-surface temperatures modeled for the Moon's south pole (85°S to pole)," Lunar and Planetary Inst., Universities Space Res. Assoc., Univ. Houston, Tech. Rep. 2216, Sep. 2019. Accessed: Apr. 12, 2023. [Online]. Available: https://repository.hou.usra.edu/handle/20.500.11753/1336

[31] E. Detsis, O. Doule, and A. Ebrahimi, "Location selection and layout for LB10, a lunar base at the lunar north pole with a liquid mirror observatory," *Acta Astronautica*, vol. 85, pp. 61–72, Apr. 2013.

[32] K. R. Enzenauer, "Energy storage and pulsed power with a lunar superconducting magnetic energy storage (SMES) system," M.S. thesis, Naval Postgraduate School, Monterey, CA, USA, Jun. 2023.

[33] M. Evans and A. Ignatiev, "Lunar superconducting magnetic energy storage (LSMES)," Lunar Surf. Innov. Consortium, Universities Space Res. Assoc., Univ. Houston. Lunar Planetary Inst., Tech. Rep. 2106, 2018, doi: 10.13140/RG.2.2.20472.08968.

[34] R. Woods-Robinson, M. A. Siegler, and D. A. Paige, "A model for the thermophysical properties of lunar regolith at low temperatures," *J. Geophys. Res., Planets*, vol. 124, no. 7, pp. 1989–2011, Jul. 2019, doi: 10.1029/2019JE005955.

[35] J. Biele, M. Grott, M. E. Zolensky, A. Benisek, and E. Dachs, "The specific heat of astro-materials: Review of theoretical concepts, materials, and techniques," *Int. J. Thermophys.*, vol. 43, no. 9, p. 144, Aug. 2022, doi: 10.1007/s10765-022-03046-5.

[36] O. Zucker, J. Wyatt, and K. Lindner, "The meat grinder: Theoretical and practical limitations," *IEEE Trans. Magn.*, vol. MAG-20, no. 2, pp. 391–394, Mar. 1984.

[37] A. Sitzman, D. Surls, and J. A. Mallick, "Design, construction, and testing of an inductive pulsed power supply for a small railgun," *IEEE Trans. Magn.*, vol. 43, no. 1, pp. 270–274. Jan. 2007.

[38] G. V. Nosov, M. G. Nosova, Y. Z. Vasil'eva, and E. O. Kuleshova, "Calculation and analysis of the power supply of a railgun from a magnetohydrodynamic generator and a transformer," *J. Appl. Mech. Tech. Phys.*, vol. 59, no. 2, pp. 251–257, Mar. 2018.

[39] *U.S. Department of Energy Announces \$10M to Develop High Performance Superconductors*, ARPA-E Press Release, Dept. Energy, Adv. Res. Projects Agency, Energy, Washington, DC, USA, May 2023.

**Ian R. McNab** (Life Fellow, IEEE) received the B.Sc. degree (Hons.) in physics from the University of Leeds, Leeds, U.K., and the Ph.D. degree from the University of Reading, Reading, U.K.

He is a Research Professor with the Naval Postgraduate School, Monterey, CA, USA. He has authored over 150 scientific papers on pulsed power, EM launch, rotating machines, current collection, and plasma- and magneto-fluid dynamics.

Dr. McNab has been on the Steering Committee of the International EM Launcher Symposia, since 1982. He was a member of the IEEE Plasma Sciences and Nuclear Committee for nine years. He received the EML Symposium's Peter Mark Medal in 1990, the Lavrentyev Medal from the Siberian Division of the Russian Academy of Sciences in 2003, and the IEEE Erwin Marx Medal in 2013.

**Kristin R. Enzenauer** received the B.S.E. degree in aerospace studies from Arizona State University, Tempe, AZ, USA, in 2017, and the M.S. degree in space systems operations and physics from the Naval Postgraduate School, Monterey, CA, USA, in June 2023 on the topic "Energy storage and pulsed power with a lunar superconducting magnetic energy storage (SMES) system."